

Rodrigo O. C. Aguiar
Emerson L. Gasparetto
Dante L. Escuissato
Edson Marchiori
Debbie J. Trudell
Parviz Haghghi
Donald Resnick

Radial and ulnar bursae of the wrist: cadaveric investigation of regional anatomy with ultrasonographic-guided tenography and MR imaging

Received: 23 October 2005
Revised: 20 January 2006
Accepted: 20 January 2006
Published online: 11 May 2006
© ISS 2006

R. O. C. Aguiar · D. J. Trudell ·
P. Haghghi · D. Resnick
Veterans Affairs Medical Center -
San Diego,
3350 La Jolla Village Drive,
San Diego, CA 92161, USA

D. L. Escuissato
Universidade Federal do Paraná,
Rua General Carneiro, 181,
Curitiba - Paraná, 80060-900, Brazil

R. O. C. Aguiar · E. L. Gasparetto ·
E. Marchiori
Universidade Federal do
Rio de Janeiro,
Brigadeiro Trompowski Av.,
Cidade Universitária,
Rio de Janeiro - RJ, 21949-900, Brazil

R. O. C. Aguiar (✉)
Av. Brasília 5474 ap 83B,
Curitiba - Paraná, 81020-010, Brazil
e-mail: aguiar.rodrigo@gmail.com
Tel.: +55-41-99141551
Fax: +55-41-32682181

Abstract *Objective:* To demonstrate the anatomy of the radial and ulnar bursae of the wrist using MR and US images. *Design:* Ultrasonographic-guided tenography of the tendon sheath of flexor pollicis longus (FPL) and the common tendon sheath of the flexor digitorum of the fifth digit (FD5) of ten cadaveric hands was performed, followed by magnetic resonance imaging and gross anatomic correlation. Patterns of communication were observed between these tendon sheaths and the radial and ulnar bursae of the wrist. *Results:* The tendon sheath of the FPL communicated with the radial bursa in 100% (10/10) of cases, and the tendon sheath of the FD5 communicated with the ulnar bursa in 80% (8/10). Communication of the radial and ulnar bursae was evident in 100% (10/10), and presented an “hourglass” configuration in the longitudinal plane. *Conclusions:* The ulnar and radial bursae often communicate. The radial bursa

communicates with the FPL tendon sheath, and the ulnar bursa may communicate with the FD5 tendon sheath.

Keywords Wrist · Flexor tendon sheath · Ulnar bursa · Radial bursa · Magnetic resonance · Anatomy

Introduction

The radial and ulnar bursae are synovium-lined structures situated in the volar region of the wrist, adjacent respectively to the tendons of the flexor pollicis longus (FPL) and flexor digitorum of the fifth digit (FD5). The ulnar bursa is composed of three invaginations (Fig. 1) that extend around the flexor tendons at the level of the carpal tunnel: (1) a superficial extension situated between the transverse carpal ligament and the flexor digitorum superficialis tendons, (2) a middle one between the flexor

digitorum superficialis tendons and the flexor digitorum profundus tendons, and (3) a deep layer, behind the flexor digitorum profundus tendons [1, 2]. The most common configuration of the ulnar and radial bursae and the flexor tendon sheaths of the fingers are well-described by Poirier [3]. Communication between the FPL tendon sheath and the radial bursa and between the FD5 tendon sheath and the ulnar bursa is typical, as is the lack of continuity of the flexor tendon sheaths of the index, long, and ring fingers with the ulnar bursa (Fig. 2). An intermediate bursa represents a common connection between the radial and

ulnar bursae [1]. Other patterns of communication are far less common [3]. These communications are of clinical importance in explaining the spread of inflammatory, infectious and even neoplastic processes that involve this region.

According to the knowledge of the authors, although these anatomic features are described, there is no study correlating these features with magnetic resonance (MR) and ultrasound (US) images. The purposes of our research are to demonstrate both the most common pattern of communication of these bursae and digital tendon sheaths and the relationship between the flexor tendons at the palmocarpal level and the radial and ulnar bursae.

Material and methods

Cadaveric and specimens preparation

Ten hands harvested from nine fresh cadavers (five men and four women, 79–97 years of age at death; mean age at death, 83.8 years) were obtained. The arms were transected 10 cm proximal to the radiocarpal joint, and immediately deep-frozen at -40°C (Forma Bio-Freezer; Forma Scientific, Marietta, OH, USA). All specimens were then allowed to thaw for 24 hours at room temperature prior to ultrasound-guided tenography and MR imaging. Radiography in the frontal and lateral projections was performed in all hands in order to exclude important traumatic or degenerative articular disorders.

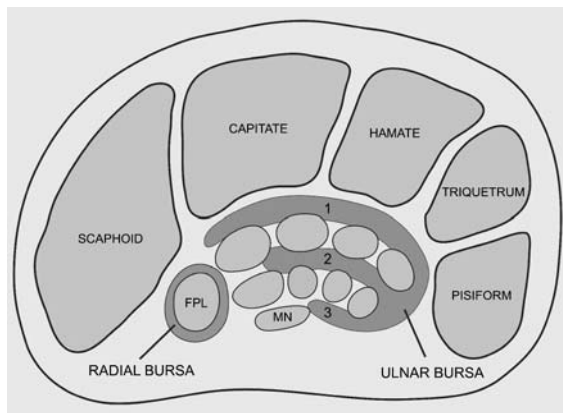


Fig. 1 Schematic drawing at the carpal level showing the invaginations of the ulnar bursa: (1) the deep layer, between the carpal bones and the flexor digitorum profundus tendons, (2) intermediate layer, between the flexor digitorum profundus tendons and flexor digitorum superficialis tendons, and (3) superficial layer, volar to the flexor digitorum superficialis tendons. *FPL*: flexor pollicis longus tendon; *MN*: median nerve

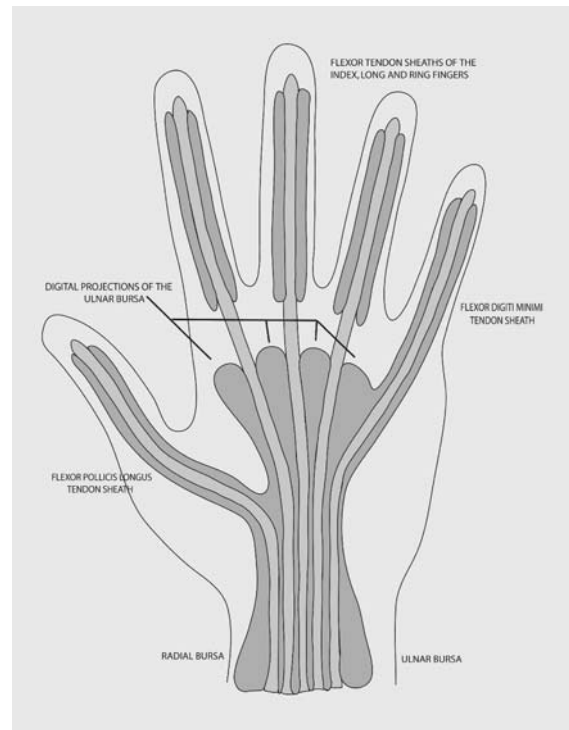


Fig. 2 Schematic drawing showing the most common pattern of communication of the ulnar and radial bursa and the flexor tendon sheaths of the fingers. Note the communication of the radial bursa and the tendon sheath of the flexor pollicis longus and the ulnar bursa and the tendon sheath of the flexor tendons of the fifth finger

US Tenography

Gray-scale US was performed by using a 14 MHz transducer (HDI 5000, Advanced Technical Laboratories, Bothell, WA, USA). This technique was used to guide the insertion of a needle during tenography of the FPL and FD5 sheaths. A 25-gauge needle was inserted through the volar skin at the level of the proximal third of the proximal phalanges, and localized just superficial to the FPL and FD5 tendons. Subsequently, approximately 5–15 ml of a solution consisting of 1 ml of gadopentate dimeglumine (Magnevist, Shering, Berlin, Germany), diluted in 250 ml of saline solution and mixed with 0.5 ml of iohexol and 0.5 ml of a mixture of gelatin and different colors (green or yellow or blue), were injected in the tendon sheaths: green solution for the FPL tendon sheath and yellow or blue solution for the FD5 tendon sheath. A yellow solution was used in the first specimen, but the correlation with the macroscopic slices was not satisfactory. In all the other specimens, a blue solution was injected in this tendon sheath, improving the correlation. US images of the wrist were obtained in the axial and sagittal planes during contrast injection, and the presence of an anechoic laminar shape image around these tendons ensured the correct location of the contrast solution. Tenography of the FPL was always performed first and followed by the injection of

the FD5 tendon sheath. The injection was stopped when the fluid returned into the syringe with release of pressure from the plunger.

MR Imaging

MR imaging was accomplished within approximately 30 minutes after the injection of the contrast agent. MR imaging was performed with a 1.5 T clinical system (Signa; GE Medical Systems, Milwaukee, WI, USA) with a dedicated phased array wrist coil. T1-weighted spin-echo images were obtained in the axial plane (500-566/11-13 [repetition time msec/echo time msec], 2.5-mm section thickness, 14×12 cm field of view). T1-weighted spin-echo with frequency-selective fat saturation were obtained in the axial plane (566/13, 2.5-mm section thickness, 14×12 cm field of view), in the sagittal plane (500-566/11-13, 2.5-mm section thickness, 12-cm field of view) and coronal plane (616-767/12, 2.5-mm section thickness, 14×12 cm field of view). T2-weighted spin-echo images were obtained in the axial plane (2900-3166/65-73, 2.5-mm section thickness, 12-cm field of view). In each plane, MR imaging was performed by using a 3-mm section thickness, a matrix size of 224×256.

Macroscopic anatomy and histology

After imaging, all specimens were deep frozen at -40 C for at least 1 day and subsequently cut with a band saw into 3 mm-thick sections that corresponded almost exactly to the thickness of the images along one of the imaging planes: Axial ($n=9$) and coronal ($n=1$) plane. The anatomic slices were cleaned with running water for macroscopic inspection. Each slice was recorded photographically to determine anatomic relationships of the bursae and correlation with MR imaging images. Two criteria were used to decide if communication of the bursae and the tendon sheath of the fingers were present: the direct visualization of the communication of these structures, and the mixture of the different colors in the location of the expected bursa. Additional photographic images were obtained using backlight, facilitating the analysis of the colors of the injected solutions. Each slice was radiographed (Faxitron; Hewlett Packard, McMinnville, OR, USA) in an attempt to depict the iodexol component of the solution; however, after the process of water irrigation of the slices, it was not possible to distinguish accurately this component of the solution and these data were not used.

Results

Communication of the FPL tendon sheath and the radial bursa was evident in all specimens ($n=10$). The FD5 tendon

sheath communicated with the ulnar bursa in 80% ($n=8$). All specimens ($n=10$) demonstrated communication of the radial and ulnar bursae (Fig. 3a-c). In two cases (20%), a sac-like structure was evident encircling the flexor tendons of the index finger, which did not communicate with its distal tendon sheath but did communicate with the ulnar and radial bursae. (Fig. 4a,b). Other patterns of tendon sheath communications were not visualized. In 100%, the deep layer of the ulnar bursa began proximally at the level of the pronator quadratus muscle and extended distally, passing the carpal transverse ligament. The superficial and intermediate layers of the ulnar bursa began more distally and terminated more proximally than the deep layer. In all cases, the radial bursa began at the level of the pronator quadratus muscle or just distal to it. Some extravasation of the contrast agent at the level of the injection site was evident in all specimens, related to the large volume of injected solution necessary to distend the bursae. On the axial MR and US images, it was possible to visualize the bursae distal and proximal to the carpal tunnel. At this level, the deep layer of the ulnar bursa was well-seen. On the coronal and sagittal MR images and the sagittal US images, the bursae filled with contrast agent, displayed a “figure of eight”, or “hourglass,” configuration with the constricted part at the level of the carpal tunnel (Fig. 5a,b).

Discussion

The ulnar and radial bursae are sac-like structures, lined with a synovial membrane, localized in the palmocarpal area. The ulnar bursa, the larger of the two, begins at the level of the distal forearm, on the surface of the pronator quadratus muscle or just distal to it, extends through the carpal tunnel, and terminates 1–3 cm proximal to the flexor tendon sheaths of the fingers [2]. It lies on the ulnar aspect of the palm, in close relation with the FD5 tendons. Previous reports indicate that the ulnar bursa is composed of: three horizontally oriented invaginations of the synovial membrane that extend around the flexor tendons, a superficial extension situated between the transverse carpal ligament and the flexor digitorum superficialis tendons, a middle one between the flexor digitorum superficialis tendons and the flexor digitorum profundus tendons, and a deep layer, behind the flexor digitorum profundus tendons [1, 2]. The superficial layer is the smallest extension, and the deep layer the largest. The space common to the three partitions is reported to be at the ulnar side, adjacent to the flexor tendons of the fifth digit [2]. The radial bursa begins at the level of the distal line of the pronator quadratus muscle or lies on the volar aspect of this muscle, and extends along the radial aspect of the wrist through the carpal tunnel, involving the FPL tendon and communicating distally with its tendon sheath [1, 2]. Communication of the ulnar and radial bursae is common, with a reported frequency of 50–85% [1, 3]. Such communication may be

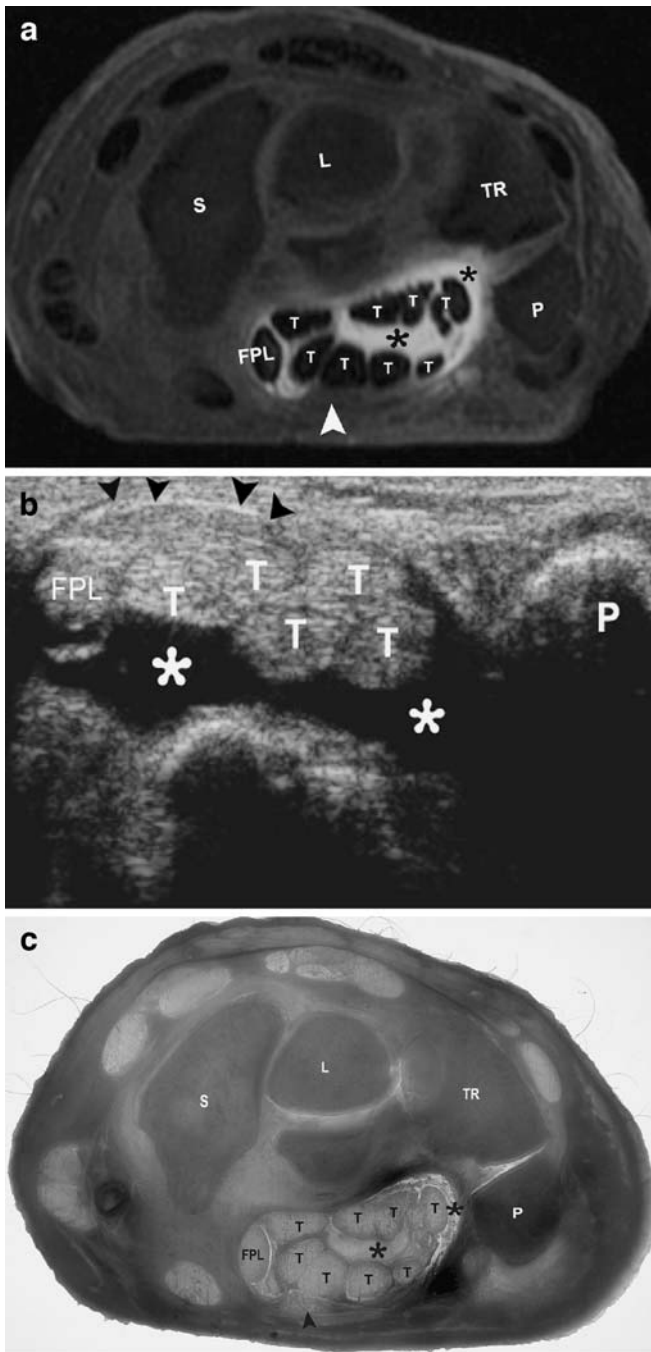


Fig. 3 a–c MR, US and cadaveric anatomy of the radial and ulnar bursae at the level of the carpal tunnel. **a** Axial (566/13) T1-weighted spin-echo MR imaging with fat saturation after tenography. **b** axial US and **c** wrist specimen, depicting the contrast (asterisks) in the radial and ulnar bursae around the flexor tendons (T) at the level of the carpal tunnel. Arrow head: median nerve, S: scaphoid, L: lunate, TR: triquetrum; P: pisiform, FPL: flexor pollicis longus tendon

through an intermediate bursa between the deepest layer of the ulnar bursa and radial bursa, behind the flexor digitorum profundus tendon of the index finger or less commonly

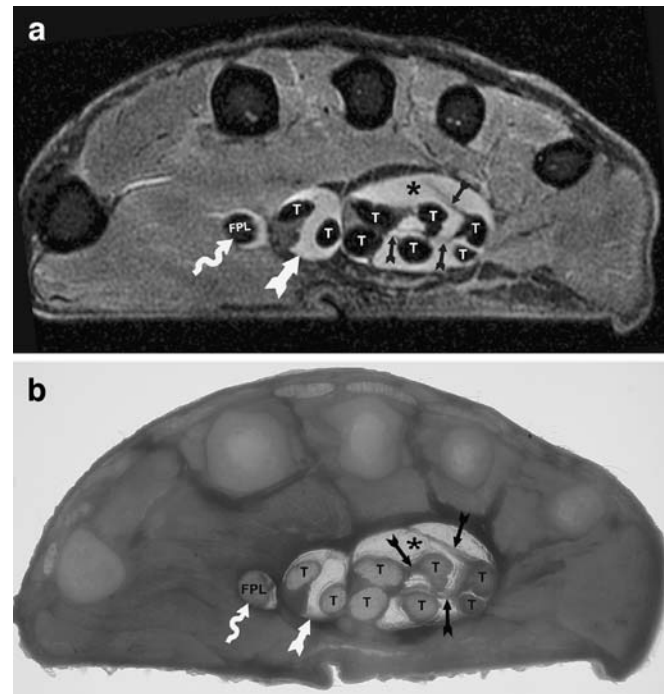
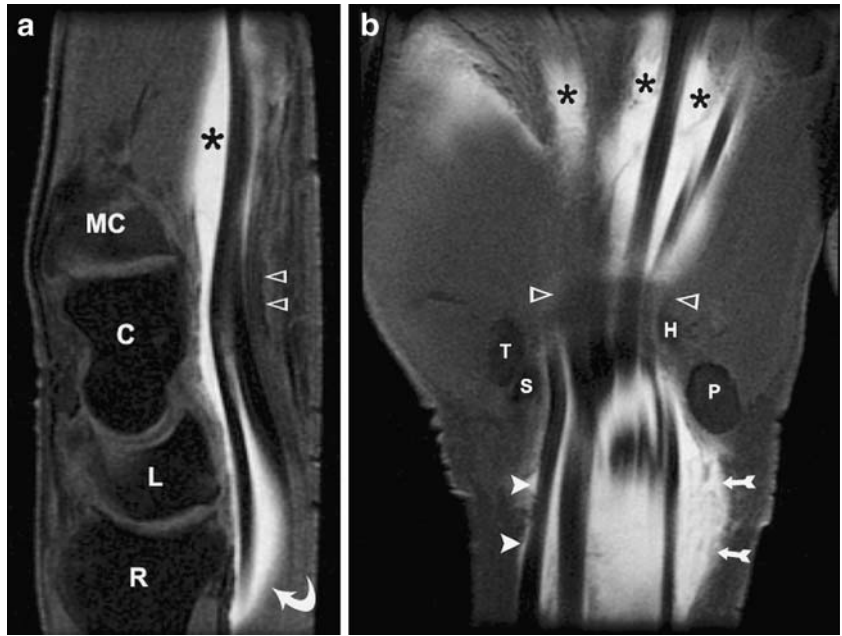


Fig. 4 a, b. MR, and cadaveric anatomy of the intermediate bursa at the level of the proximal metacarpal bones. **a** Axial (2900/65) T2-weighted spin-echo, **b** specimen, depicting the intermediate bursa (white arrow), between the radial and ulnar bursae. Curved arrow: tendon sheath of the flexor pollicis longus (FPL), black arrows: strands of tissue connecting the flexor tendons (T), asterisk: contrast agent in the ulnar bursa

between the flexor tendons (superficialis and profundus) of the index finger [1]. Although the radial bursa always communicates with the FPL tendon sheath [1–3], the ulnar bursa communicates with the FD5 tendon sheath in about 50% to 80% of wrists [1, 3]. Other less frequent patterns are also described. A statistical analysis of tendon sheath patterns in the hand, using air inflation technique in 367 cases, demonstrated that the ulnar bursa communicates with the tendon sheaths of the index finger in 5.1%, long finger in 4%, and ring finger in 3.5% of cases [3]. Other research has shown a separate carpal tendon sheath, without communication with either the radial or ulnar bursa, enveloping the flexor tendons of the index finger [3].

Our work demonstrated the most common patterns of communication of the radial and ulna bursae and the flexor tendon sheaths of the fingers and thumb, as well as the landmarks of these bursae. All specimens demonstrated communication between the radial bursa and the FPL tendon sheath. The radial bursa began proximally at the distal margin of the pronator quadratus muscle. The ulnar bursa was seen in all cases, starting at the level of the distal volar surface of the pronator quadratus muscle. It communicated in all cases with the radial bursa, a higher frequency than reported previously [1, 3]. This may relate to the amount of injected contrast agent that we used. On the coronal and the sagittal planes, the carpal bursae had a

Fig. 5 a, b. Typical appearance of the radial and ulnar bursae in the sagittal and coronal planes. **a** Sagittal (500/13) and **b** coronal (616/12) T1-weighted spin-echo MR imaging with fat saturation after tenography, demonstrating the “hour-glass” or “figure of eight” configuration of the ulnar and radial bursae as well as the proximal and distal limits of it. Note the narrowing at the level of the carpal tunnel. *White arrowheads*: radial bursa, *arrows*: ulnar bursa, *curved arrow*: proximal portion of the ulnar bursa, *asterisks*: distal extensions of the ulnar bursa around the flexor tendons, *open arrowheads*: transverse carpal ligament. *MC*: metacarpal bone, *C*: capitate, *L*: lunate, *R*: radius, *T*: trapezoid, *S*: scaphoid, *H*: hook of hamate, *P*: pisiform



“figure of eight”, or “hourglass”, shape, with the constricted part situated at the level of the carpal tunnel. This shape has been previously described in cases of infectious or inflammatory lesions of the bursae [4–7].

There are some limitations to this study, including the advanced age (83 years) of persons from whom the specimens were derived, which could have increased the incidence of degenerative communications; a small number of specimens, in which findings may not reflect the true incidence of communications; and the injection of a considerable amount of contrast agent in order to distend

the bursae, which could have led to an overestimation of the frequency of communication. Despite these limitations, however, the most common patterns of communication between the radial and ulnar bursae and the flexor tendon sheaths of the fingers have been demonstrated. This is of clinical importance in explaining the patterns of spread of inflammatory, infectious and even neoplastic processes that involve this region. When inflamed, bursitis, rather than tenosynovitis, is the correct term when describing changes of the synovial tissue within the carpal tunnel.

References

1. Resnick D. Roentgenographic anatomy of the tendon sheaths of the hand and wrist: tenography. *Am J Roentgenol Radium Ther Nucl Med* 1975; 124:44–51
2. Kaplan E. The retinacular system of the hand. In: *Functional and surgical anatomy of the hand*. 3rd edition. Philadelphia: J.B. Lippincott; 1965. pp 277–279
3. Scheldrup E. Tendon sheath patterns in hand. *Modern Med* 1952;20:92–93
4. Hsu CY, Lu HC, Shih TT. Tuberculous infection of the wrist: MRI features. *AJR Am J Roentgenol* 2004; 183:623–628
5. Jaovisidha S, Chen C, Ryu KN, et al. Tuberculous tenosynovitis and bursitis: imaging findings in 21 cases. *Radiology* 1996;201:507–513
6. Chau CL, Griffith JF, Chan PT, Lui TH, Yu KS, Ngai WK. Rice-body formation in atypical mycobacterial tenosynovitis and bursitis: findings on sonography and MR imaging. *AJR Am J Roentgenol* 2003;180:1455–1459
7. Padula A, Salvarani C, Barozzi L, et al. Dactylitis also involving the synovial sheaths in the palm of the hand: two more cases studied by magnetic resonance imaging. *Ann Rheum Dis* 1998;57:61–62